Pharmacological Research 141 (2019) 189–200

Contents lists available at ScienceDirect

Pharmacological Research

journal homepage: www.elsevier.com/locate/yphrs

Topiramate protects apoE-deficient mice from kidney damage without affecting plasma lipids

Stefano Manzini[a,1], Marco Busnelli[a,1], Cinzia Parolini[a], Lucia Minoli[b,c], Alice Ossoli[d], Elena Brambilla[a], Sara Simonelli[d], Eftychia Lekka[e], Andreas Persidis[e], Eugenio Scanziani[b,c], Giulia Chiesa[a,*]

[a] Department of Pharmacological and Biomolecular Sciences, Università degli Studi di Milano, via Balzaretti 9, 20133 Milano, Italy
[b] Department of Veterinary Medicine, Università degli Studi di Milano, via Celoria 10, 20133 Milano, Italy
[c] Mouse & Animal Pathology Laboratory (MAPLab), Fondazione UniMi, viale Ortles 22/4, 20139 Milano, Italy
[d] Center E. Grossi Paoletti, Department of Pharmacological and Biomolecular Sciences, Università degli Studi di Milano, via Balzaretti 9, 20133 Milano, Italy
[e] Biovista, 34 Rodopoleos Street Ellinikon, Athens 16777, Greece

ARTICLE INFO

Keywords:
Topiramate
apoE-deficient mice
Cholesterol
Atherosclerosis
Foam cells
Glomerular lipidosis

ABSTRACT

Topiramate is an anticonvulsant drug also prescribed for migraine prophylaxis that acts through several mechanisms of action. Several studies indicate that topiramate induces weight loss and a moderate reduction of plasma lipids and glucose. Based on these favourable metabolic effects, aim of this study was to evaluate if topiramate could modulate atherosclerosis development and protect target organs of dysmetabolic conditions.

Thirty apoE-deficient mice were divided into three groups and fed for 12 weeks a high fat diet (Control) or the same diet containing topiramate at 0.125% and 0.250%. Body weight, water and food intake were monitored throughout the study. Plasma lipids and glucose levels were measured and a glucose tolerance test was performed. Atherosclerosis development was evaluated in the whole aorta and at the aortic sinus. Histological analysis of liver, kidney and adipose tissue was performed.

Topiramate did not affect weight gain and food intake. Glucose tolerance and plasma lipids were not changed and, in turn, atherosclerosis development was not different among groups. Topiramate did not modify liver and adipose tissue histology. Conversely, in the kidneys, the treatment reduced the occurrence of glomerular lipidosis by decreasing foam cells accumulation and reducing the expression of inflammatory markers. Blood urea nitrogen levels were also reduced by treatment.

Our results indicate that topiramate does not affect atherosclerosis development, but preserves kidney structure and function. The study suggests that topiramate could be investigated in drug repurposing studies for the treatment of glomerular lipidosis.

What is already known

- Topiramate lowers body weight and moderately reduces plasma lipids and glucose levels
- Glomerular lipidosis associates to dyslipidemic conditions prone to the development of kidney disease

What this study adds

- Topiramate does not affect atherosclerosis progression in apoE-deficient mice
- Topiramate protects the kidneys of apoE-deficient mice from developing glomerular lipidosis

Abbreviations: apoE, apolipoprotein E; FDA, Food and Drug Administration; WAT, white adipose tissue; BAT, brown adipose tissue; TC, total cholesterol; TG, triglycerides; PL, phospholipids; FPLC, fast protein liquid chromatography; LDL, low density lipoprotein; VLDL, very low density lipoprotein; BUN, blood urea nitrogen; Tgfb1, transforming growth factor beta 1; Il6, interleukin-6; Ccl2, C-C motif chemokine ligand 2; MCP-1, monocyte chemoattractant protein 1; LCAT, lecithin–cholesterol acyltransferase; Iba-1, ionized calcium binding adaptor molecule 1; CD3, cluster of differentiation 3; DAB, 3,3'-diaminobenzidine; O.R.O., Oil Red O

* Corresponding author.
E-mail address: giulia.chiesa@unimi.it (G. Chiesa).
[1] These authors equally contributed to this work.

https://doi.org/10.1016/j.phrs.2018.12.022
Received 12 September 2018; Received in revised form 16 November 2018; Accepted 24 December 2018
Available online 26 December 2018

Clinical Significance

- Topiramate could be considered as a drug repurposing strategy for the treatment of glomerular lipidosis

1. Introduction

Topiramate is a drug initially marketed for the treatment of epilepsy [1,2] that over the years showed therapeutic effects also in a number of neurological conditions such as pain syndromes [3,4] and movement disorders [5], and it was approved for migraine prophylaxis in 2004 [6]. The variety of possible clinical applications is consistent with the multiple mechanisms of action, that include the blockade of voltage-gated sodium channels, enhancement of GABA receptor activity, inhibition of glutamate receptors, inhibition of L-type voltage-gated calcium ion channels and inhibition of carbonic anhydrases [7–9]. As for several antiepileptic drugs, topiramate has been shown to cause weight loss, through mechanisms that include reduced food intake and altered efficiency of energy utilization [10]. Topiramate treatment has been also shown, in experimental and clinical studies, to induce other favourable metabolic changes, such as a moderate reduction of plasma lipids, lower glycaemia and increased insulin sensitivity [11,12]. The combination of weight loss and metabolic improvements by topiramate treatment led the FDA to approve in 2012 the combination phentermine-topiramate extended release for the long-term treatment of obesity [13].

The multiple metabolic effects exerted by topiramate raise the question of whether this drug could favourably affect cardiovascular disease. To this aim, in the present work, topiramate was administered at two different doses to apolipoprotein E (apoE)-deficient mice, and a possible effect on atherosclerosis development, as well as on target organs of dysmetabolic conditions, was evaluated. Topiramate treatment did not alter plasma lipids and glucose levels, nor affect the extent of atherosclerosis. Interestingly, it displayed a marked protective effect on kidney by reducing the glomerular lipidosis observed in controls.

2. Methods

2.1. Animals, diet and pharmacological treatment

Procedures involving animals and their care were conducted in accordance with institutional guidelines that are in compliance with national (D.L. No. 26, March 4, 2014, G.U. No. 61 March 14, 2014) and international laws and policies (EEC Council Directive 2010/63, September 22, 2010: Guide for the Care and Use of Laboratory Animals, United States National Research Council, 2011). The experimental protocol was approved by the Italian Ministry of Health (Protocollo 428/2015-PR).

Thirty apoE knockout female mice (strain 002052), aged 8 weeks, were purchased from Charles River Laboratories (Calco, Italy) and housed at constant temperature and relative humidity. Scobis Uno, a vegetable bedding made of wood particles obtained from spruce, was used. Mice were randomized into three experimental groups (n = 10) and fed for 12 weeks a high-fat diet (adjusted calories 42% from fat, 0.2% cholesterol) without supplementation (Control), or supplemented with topiramate 0.125% w/w (T-low) or 0.250% w/w (T-high). Mice were house 3–4 per cage, n = 3 cages per group.

2.2. Plasma and tissue harvesting

Blood was collected before and at the end of dietary treatment, after 5 h fast, as described [14]. Plasma was separated by centrifugation for 10 min at 5900 × g at 4 °C.

At the end of the experimental period, mice were anesthetized with 2% isoflurane and blood was removed by perfusion with PBS [15]. Aorta was rapidly harvested as described [16], longitudinally opened, pinned flat on a black wax surface in ice-cold PBS and photographed unstained for plaque quantification (see below). Hearts were removed, fixed in 10% formalin for 24 h, then transferred into PBS containing 30% sucrose (w/v) for 24 h at 4 °C before being embedded in OCT compound and stored at −80 °C.

Liver, abdominal white adipose tissue (WAT), brown adipose tissue (BAT) and kidneys were either snap-frozen in liquid nitrogen for subsequent molecular analyses, or immersion-fixed in 10% formalin for 24 h, then transferred in 70% ethanol and processed for histological analyses as described [14].

2.3. Plasma measurements and glucose tolerance test

Plasma total cholesterol (TC), triglycerides (TG) and phospholipids (PL) were measured with enzymatic methods. Quantitative determination of urea nitrogen in plasma (BUN) and creatinine was assayed by immunoenzymatic method with the Roche Cobas c311 system.

For the glucose tolerance test, mice were injected, after 5 h fast, with 2 g/Kg glucose via i.p. injection of 20% w/v sterile glucose solution in PBS. Glucose levels were determined using the One touch Ultra glucometer every 30 min.

2.4. En face analysis, histology and immunohistochemistry

2.4.1. En face

Aorta images were captured with a stereomicroscope-dedicated camera (IC80 HD camera, MZ6 microscope, Leica Microsystems, Germany), and analysed with ImageJ image processing program [17]. Atherosclerosis extent was quantified by two independent operators blinded to the dietary treatments.

2.4.2. Aortic sinus histology

Serial cryosections (7 µm thick) of the aortic sinus were cut. Approximately 25 slides with 3 cryosections per slide were obtained, spanning the three cusps of the aortic valves. Every sixth slide was stained with hematoxylin and eosin (H&E) to detect plaque area, calculated as the mean area of those sections showing the three cusps of the aortic valves. Foam cells were quantified as described [18] and expressed as percent area over total plaque area. Adjacent slides were stained with Oil red O (O.R.O.) to detect intraplaque neutral lipids. Macrophages were detected using an anti-Mac2 antibody. The detection was performed using an ImmPRESS reagent kit, 3,3′-diaminobenzidine was used as the chromogen and the sections were counterstained with Gill's haematoxylin. The Nanozoomer S60 (Hamamatsu Photonics, Japan) scanner was used to acquire digital images that were subsequently processed with the NDP.view2 software (Hamamatsu Photonics, Japan). A blinded operator to dietary treatments quantified plaque size and composition.

2.4.3. Liver, abdominal WAT, BAT, spleen, kidney histology/immunohistochemistry

Formalin fixed organs/tissues were dehydrated in a graded scale of ethanol, and paraffin embedded. Serial sections (5 µm thick) were cut and stained with H&E. In addition, to investigate the presence of inflammatory cells in kidney and liver, macrophages and T lymphocytes were detected using an anti-Iba1 antibody and an anti-CD3 epsilon antibody. The specific binding of the primary antibodies was visualized by the avidin-biotin-peroxidase (ABC) procedure with a commercial immunoperoxidase kit (Vectastain Standard Elite), using 3,3′-diaminobenzidine substrate (DAB) as chromogen and Mayer's hematoxylin as counterstain. Images were acquired with a DFC310 FX camera on a DM2500 microscope (Leica Microsystems, Germany).

Hepatic inflammatory infiltrates were classified considering the distribution (perivascular or parenchymal) and quantified according the following classes: small (S): less than 10 cells, medium (M): 11–100 cells, large (L): > than 100 cells. The presence of subendothelial foamy

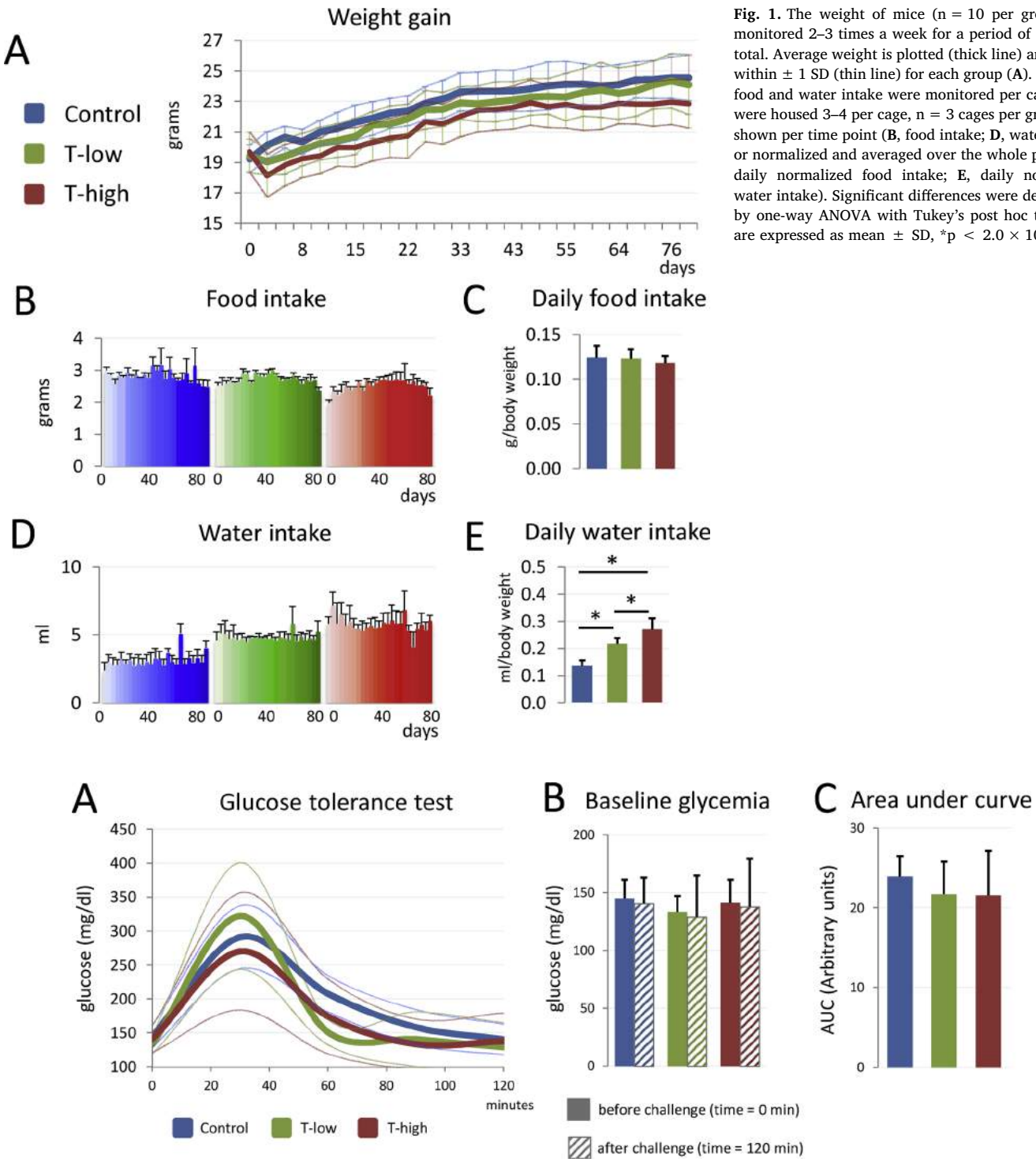

Fig. 1. The weight of mice (n = 10 per group) was monitored 2–3 times a week for a period of 12 weeks total. Average weight is plotted (thick line) and shown within ± 1 SD (thin line) for each group (**A**). Likewise, food and water intake were monitored per cage (mice were housed 3–4 per cage, n = 3 cages per group) and shown per time point (**B**, food intake; **D**, water intake) or normalized and averaged over the whole period (**C**, daily normalized food intake; **E**, daily normalized water intake). Significant differences were determined by one-way ANOVA with Tukey's post hoc test. Data are expressed as mean ± SD, *$p < 2.0 \times 10^{-5}$.

Fig. 2. After i.p. injection of 2 g/Kg glucose (n = 5 per group), glycaemia was monitored at intervals of 30 min, up to 120 min total. Glucose concentration as function of time is shown (thick line), within ± 1 SD (thin line) for each group (**A**). Baseline glucose levels are charted before (time = 0 min, solid bars) and after (time = 120 min, striped bars) the glucose tolerance test (**B**). Measurements of areas under the curve (AUC) are shown in **C**, in arbitrary units. Data are expressed as mean ± SD.

macrophage aggregates in the liver was scored as follows: 0: no aggregates, 1: 1–3 aggregates, 2: 4–10 aggregates, 3: > 10 aggregates.

Hepatic glycogen accumulation and steatosis were scored as follows: 0: absent, 1: slight, 2: moderate, 3: severe.

The severity of glomerular lipidosis in the kidney was scored as follows: 0: absent, 1: < 3 glomeruli affected, 2: 4–10 glomeruli affected, 3: > 10 glomeruli affected. Tubular necrosis was scored as present (1) or absent (0). All histological and immunohistochemichal features were assessed by an operator blinded to dietary treatments.

2.5. RNA extraction and cDNA synthesis

Total RNA was isolated from mouse tissues using the NucleoSpin RNA extraction kit according to the manufacturer's instructions, with on-column DNA digestion. RNA concentration and purity were checked, and 1 μg RNA was retrotranscribed to cDNA, as described [19]. Possible

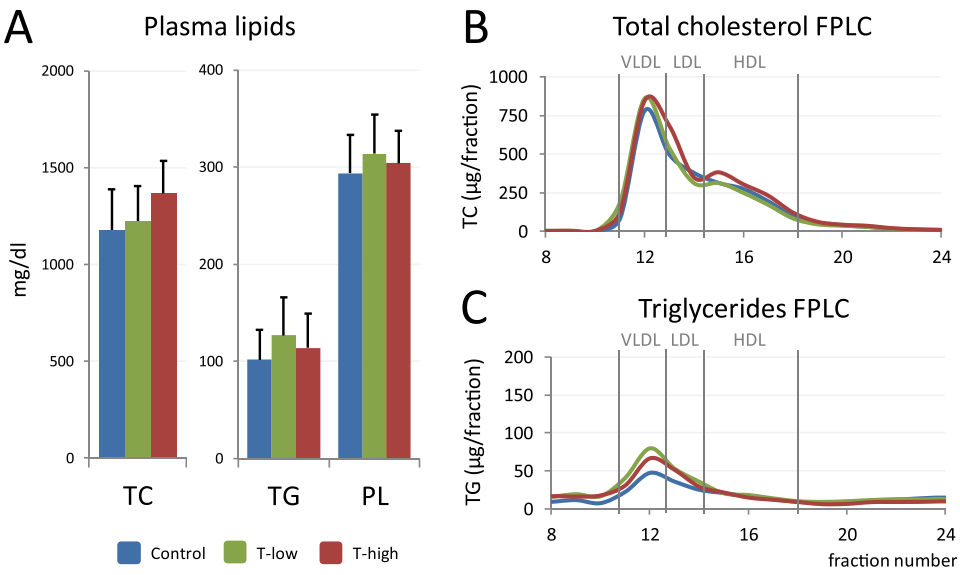

Fig. 3. Total cholesterol (TC), triglyceride (TG) and phospholipid (PL) levels (n = 10 per group), quantified after 5 h fasting, are shown (**A**). TC and TG distributions among plasma lipoproteins by FPLC are shown in **B** and **C**, respectively. Each profile was obtained from pooled plasma of all mice within each experimental group (n = 10). Data are expressed as mean ± SD.

gDNA contamination was ruled out by running a PCR on 20 ng of cDNA/RNA with a primer pair producing two amplicons of different size on cDNA (193 bp) and gDNA (677 bp). Conditions as follows: 95 °C for 3 min, followed by 35 cycles of 30 s at 95 °C, 30 s at 58.5 °C, 45 s at 72 °C for 45", followed by a final amplification step of 5 min at 72 °C, with primers mmu_Srp14_f: 5'-GGAGGCTTCTGCTGACGGCG-3' and mmu_Srp14_r: 5'- GGGCTCGAGGCCCTCCACA-3'.

2.6. Quantitative PCR

20 ng of cDNA were used as template for each qPCR reaction, performed on a CFX Connect thermal cycler with iTAQ Universal Sybr Green Supermix. Standard fast cycling conditions were used, with 300 nM primer pairs listed in Supplementary Table 1. A final melting curve analysis was always included. Fold changes relative to Control group were calculated with the ΔΔCt method [20]. The housekeeping gene cyclophilin A (Ppia) was chosen as reference gene, as it is among the most stable in the kidney tissue [21].

2.7. Statistical analyses

Data are expressed as mean ± SD. Group differences were tested for statistical significance by analysis of variance (ANOVA) for repeated measurements or by one-way ANOVA, followed by Dunnett's or Tukey post hoc test. Liver and kidney histological features were analysed by the nonparametric Kruskal-Wallis test, followed by the Conover-Iman post hoc test. Tubular necrosis incidence was evaluated with a 3 × 2 chi-square test of independence. Statistical analyses were performed using the SYSTAT software (Version 13; Systat Software, Inc., Chicago, IL).

2.8. Materials

Item	Type	Supplier	City	Country
Scobis Uno	Animal bedding	Mucedola	Settimo Milanese	Italy
Adjusted calories 42% from fat, 0.2% cholesterol	Animal diet	Mucedola	Settimo Milanese	Italy
anti-CD3 epsilon antibody - COD sc-1127	Antibody	Dako	Carpinteria	USA
anti-Iba1 antibody - COD 019-19741	Antibody	Wako Chemicals	Richmond	USA
anti-Mac2 antibody - COD CL8942	Antibody	Cederlane	Ontario	Canada
Cholesterol assay - COD CP A11 A01634	Assay/Kit	ABX Diagnostics	Montpellier	France
ImmPRESS HRP Anti-Rat IgG Polymer Detection Kit MP-7404	Assay/Kit	Vector Laboratories	Burlingame	USA
iTAQ Universal Sybr Green Supermix	Assay/Kit	Bio-Rad	Segrate	Italy
NucleoSpin RNA extraction kit	Assay/Kit	Macherey-Nagel	Duren	Germany
Phospholipids assay	Assay/Kit	B.L. Chimica	Concorezzo	Italy
Tryglycerides assay - COD CP A11 A01640	Assay/Kit	ABX Diagnostics	Montpellier	France
Vectastain Elite ABC-Peroxidase Staining kit	Assay/Kit	Vector Laboratories	Burlingame	USA
3,3'-diaminobenzidine substrate (DAB)	Chemical	Vector Laboratories	Burlingame	USA
Eosin Y alcoholic solution	Chemical	Bio-Optica	Milan	Italy
Ethanol	Chemical	Sigma-Aldrich	Missouri	USA
Gill's hematoxylin	Chemical	Bio-Optica	Milan	Italy
Glucose	Chemical	Sigma-Aldrich	Missouri	USA
Mayer's hematoxylin	Chemical	Bio-Optica	Milan	Italy
OCT	Chemical	Sakura Finetek	Alphen aan den Rijn	The Netherlands
Oil red O (O.R.O.)	Chemical	Sigma-Aldrich	Missouri	USA
PBS	Chemical	Sigma-Aldrich	Missouri	USA
Sucrose	Chemical	Sigma-Aldrich	Missouri	USA
Isoflurane	Drug	Merial Animal Health	Woking	UK
Topiramate	Drug	TCI	Zwijndrecht	Belgium
Ultra touch glucometer	Instrument	LifeScan Italy	Milan	Italy

3. Results

3.1. Topiramate did not affect weight gain and food intake, but increased water intake

At randomization (day 0), mice weighed 19.2 ± 0.9 g (Control), 19.4 ± 1.1 g (T-low) and 19.6 ± 1.3 g (T-high), with p = 0.66. The growth curve of the three groups during the experimental protocol is shown in Fig. 1A. No significant differences in weight gain were

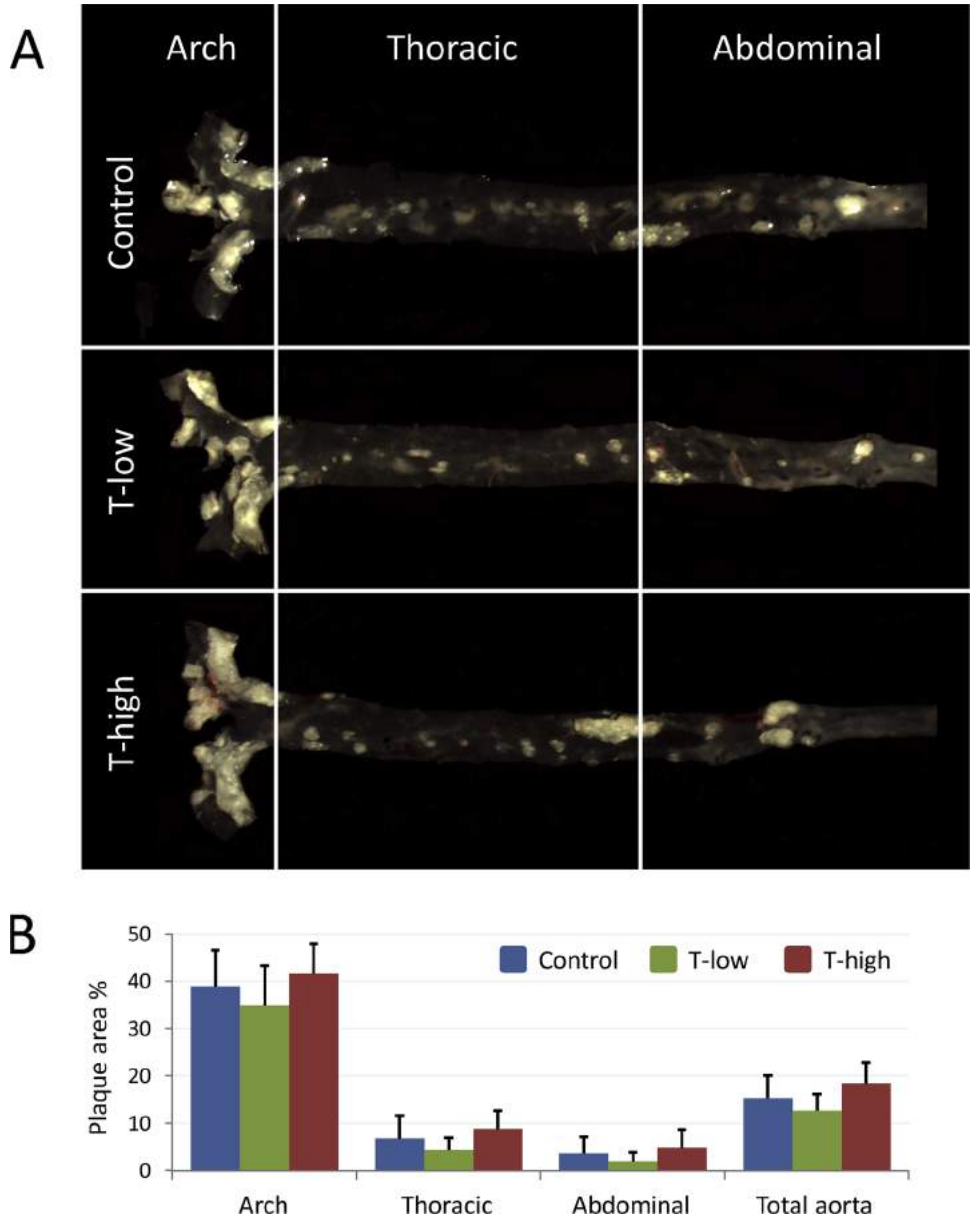

Fig. 4. Representative images of aorta from Control, T-low and T-high groups, obtained by the en face method. The aorta is cut lengthwise and pinned flat onto a black wax surface, then the exposed plaques are quantified as a percentage of the whole aortic area (**A**). Plaque extent, reported as percentage of the whole area, for aortic arch, thoracic aorta, abdominal aorta and total aorta. Data are expressed as mean ± SD (**B**).

observed among groups, although, starting from day 4 until the end of the study, the mean weight of T-high mice remained moderately lower than that of Control. Food and water intake were periodically monitored (Fig. 1B, D). Daily food intake was comparable within groups: 0.124 ± 0.01 g/g body weight in Control, 0.123 ± 0.01 g/g in T-low and 0.118 ± 0.00 g/g in T-high, with p = 0.77 (Fig. 1C). On the contrary, the overall normalized daily water intake increased linearly with the topiramate concentration, from 0.136 ± 0.01 ml/g body weight of Control, to 0.217 ± 0.02 ml/g of T-low and 0.270 ± 0.03 ml/g of T-high (Fig. 1E).

3.2. Topiramate treatment did not influence glucose tolerance

At baseline, after 5 h fast, groups did not differ in blood glucose levels that were 145.2 ± 16.2 mg/dl in Control, 133.6 ± 13.8 mg/dl in T-low and 141.4 ± 19.9 mg/dl in T-high, p = 0.55 (Fig. 2A and B). Groups responded similarly to the glucose challenge administered as i.p. injection of 2 g/Kg glucose, and differences failed to reach statistical significance at any given time point (Fig. 2A), as well as when considering the area under the curve (AUC, Fig. 2C). After peaking at ˜30 min, glucose levels returned steadily to baseline values, i.e. plasma levels measured before the glucose challenge (Fig. 2A and B).

3.3. Plasma lipids and lipid distribution were unchanged by topiramate treatment

At the end of treatment, plasma lipid concentrations were measured after 5 h fasting. Plasma total cholesterol (TC) levels moderately increased after T-high treatment (+16.3% vs Control), averaging at 1177.2 ± 211.8 mg/dl in Control, 1123.6 ± 182.4 mg/dl in T-low and 1369.2 ± 166.31 mg/dl in T-high. However, no statistically significant differences were detected among groups (p > 0.05, Fig. 3A). FPLC analysis did not show any relevant difference in cholesterol distribution among lipoprotein classes (Fig. 3B). Triglyceride (TG) levels showed a slight, non significant, increase in topiramate-treated groups compared with Control, averaging at 101.6 ± 30.8 mg/dl,

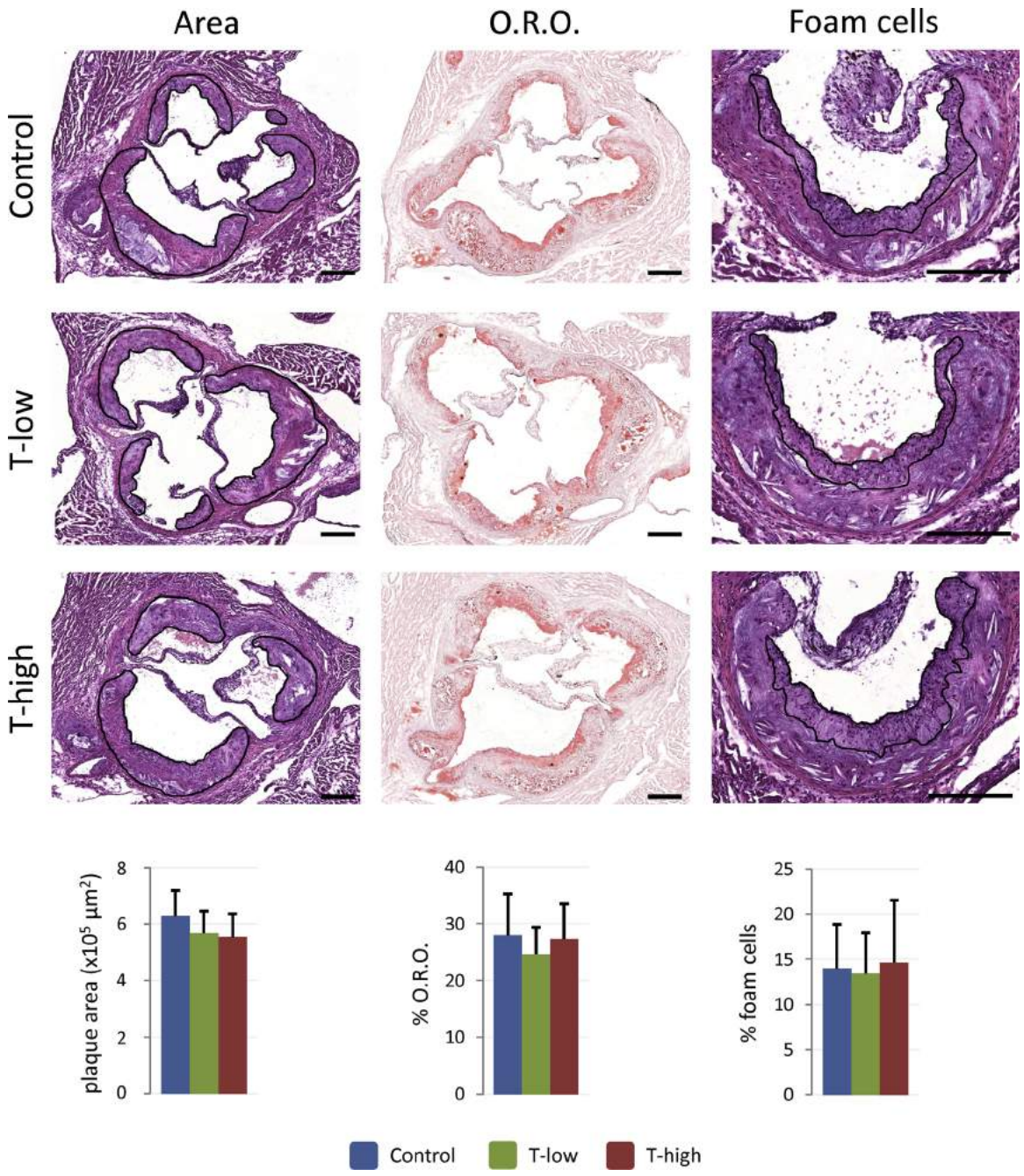

Fig. 5. Representative H&E and O.R.O. photomicrographs of aortic sinuses (top). Atherosclerotic plaque area, percentage of O.R.O.-positive plaque area and percentage of plaque occupied by foam cells were quantified and results were comparable among groups (bottom). Data are expressed as mean ± SD. Bar length = 250 µm.

126.6 ± 39.2 mg/dl and 113.5 ± 35.2 mg/dl in Control, T-low and T-high groups, respectively (Fig. 3A, p = 0.32). This slight difference was due to a higher TG content in the fractions corresponding to the VLDL peak (Fig. 3C). Last, phospholipids showed comparable levels, with 293.6 ± 39.7 mg/dl in Control, 313.6 ± 40.0 mg/dl in T-low and 303.9 ± 32.9 mg/dl in T-high (Fig. 3A).

3.4. Topiramate did not influence atherosclerosis development

Atherosclerotic plaque development was measured on aortas cut lengthwise, as percentage of area occupied by plaques, in the three aortic districts: aortic arch, thoracic and abdominal aorta. Plaque development in treated groups was not different from that in Control, both considering the aortic segments separately and the total aorta (Fig. 4A and B). In this latter case, mean values were 15.3 ± 4.8% in Control, 12.7 ± 3.4% in T-low and 18.5 ± 4.3% in T-high, with p = 0.18. Plaque extent was further quantified at the aortic sinus (Fig. 5), but likewise we did not find any statistically significant difference. Plaque area was $6.3 \times 10^5 \pm 0.9 \times 10^5$ µm^2, $5.7 \times 10^5 \pm 0.7 \times 10^5$ µm^2 and $5.5 \times 10^5 \pm 0.8 \times 10^5$ µm^2 in Control, T-low and T-high, respectively, with p = 0.17 (Fig. 5). Likewise, there were no significant differences in the accumulation of neutral lipids, quantified with O.R.O. staining among experimental groups (28.0 ± 7.2% in Control, 24.6 ± 4.8% in T-low and 27.3 ± 6.1% in T-high with p = 0.44) (Fig. 5). Foam cells quantified in the aortic sinus failed to show significant differences within groups (14.0 ± 4.9% in Control, 13.4 ± 4.5% in T-low and

Table 1
Liver histological features.

	Perivasal			Parenchymal			Glycogen	Steatosis	Subendothelial macrophages
	Inflammatory infiltrates			Inflammatory infiltrates					
	S	M	L	S	M	L			
Control	0	1	0	3	1	0	1	0	1
	1	0	0	3	0	0	0	0	1
	2	2	0	3	2	0	0	1	0
	1	1	0	3	1	0	2	0	1
	1	0	0	3	0	0	0	1	0
	0	1	0	3	1	0	0	0	0
	1	1	0	3	1	0	2	2	1
	1	0	0	2	0	0	1	0	0
	1	1	0	3	1	0	1	0	0
T-low	0	0	0	3	2	0	1	0	0
	1	0	0	2	0	0	0	0	1
	1	0	0	2	1	0	1	1	0
	1	1	0	3	2	0	1	0	0
	1	1	0	3	0	0	0	1	1
	1	0	0	3	0	0	1	1	0
	1	0	0	3	1	0	1	1	0
	1	0	0	3	1	0	2	0	0
	0	0	0	3	1	0	0	0	0
	1	2	0	3	1	0	1	2	1
T-high	1	1	0	3	2	0	1	1	1
	1	1	1	3	1	0	1	0	0
	1	0	0	3	1	0	1	1	0
	1	0	0	3	1	0	1	0	1
	1	0	0	3	1	0	1	0	0
	2	1	0	3	0	0	0	0	1
	1	1	0	2	0	0	0	1	0
	1	1	0	3	1	0	2	3	0
	0	0	0	3	1	0	1	0	0
	1	0	0	3	2	0	0	2	0

In the liver, the number of small (S: less than 10 cells), medium (M: 11–100 cells) and large (L: 101 or more cells) inflammatory infiltrates was counted per area, and ranked as follows: 0 (no infiltrate), 1 (1–3 infiltrates), 2 (4–10 infiltrates), 3 (more than 10 infiltrates). Glycogen accumulation and steatosis were given an arbitrary score, either 0 (absent), 1 (slight), 2 (moderate) or 3 (severe). The presence of large foamy macrophage aggregates in the subendothelial space or near the centrolobular vein was given a score of 1, 0 otherwise.

14.6 ± 6.9% in T-high, with p = 0.9) (Fig. 5). In addition, a macrophage-specific immunohistochemical staining did not highlight differences among group (29.0 ± 3.7% in Control, 31.2 ± 4.6% in T-low and 33.6 ± 3.2% in T-high, with p = 0.07) (Supplementary Fig. 4).

3.5. Topiramate treatment did not promote significant changes in liver, abdominal WAT and in BAT

Liver weight at sacrifice was comparable among groups, being 1.45 ± 0.20 g in Control, 1.58 ± 0.15 g in T-low and 1.58 ± 0.14 g in T-high, respectively (Supplementary Fig. 1). Similarly, no significant differences were observed in abdominal WAT, spleen, heart and kidneys (Supplementary Fig. 1).

Representative histology of liver, abdominal WAT and BAT is shown in Supplementary Fig. 2. Histological analysis of liver showed, as expected, that the high-fat diet caused an accumulation of both lipids and glycogen that was not modified by topiramate treatment (Table 1). Similarly, the amount of subendothelial foamy macrophages and inflammatory cell aggregates was comparable in the topiramate-treated groups and in Control (Table 1 and Supplementary Fig. 3). In addition, both abdominal WAT and BAT histology were unaffected by topiramate treatment (data not shown).

3.6. Topiramate treatment prevented glomerular lipidosis

Histological analysis of kidneys showed in Control the strong presence of glomerular lipidosis, identified by the presence of large foam cells within the glomerulus (Fig. 6A). Iba-1 immunostaining proved the macrophagic origin of the foam cells (Fig. 6G and J). Interestingly, a significantly lower glomerular lipidosis was observed in topiramate-treated groups vs Control (p = 0.00057, Control vs T-low; p = 0.00014, Control vs T-high) (Fig. 6B-H-K, and C-I-L), with a trend towards a dose-response effect (Table 2). No significant differences were however found between T-low and T-high (p = 0.49). No differences in the number of macrophages infiltrating the renal parenchyma outside the glomeruli were observed (data not shown). The number of infiltrating T lymphocytes, although not significant, appeared higher in Control (Fig. 6).

Tubular necrosis (defined by the presence of hyaline eosinophilic material in the tubular lumen), often associated with regenerative hyperplasia (tubular cells with basophilic cytoplasm and a large nucleus with a prominent nucleolus), was identified in 3 Controls out of 9 analysed (33.3%). Although not significant, in treated groups the incidence of tubular necrosis/hyperplasia was reduced, being present in only 1 out of 10 kidneys analysed in T-low (10%), and totally absent in the T-high group (0%) (Fig. 6 and Table 2).

BUN and creatinine levels were assessed in mouse plasma to evaluate kidney functionality. In accordance with the histological findings, BUN levels were lower in topiramate-treated mice, again in a dose-dependent manner, even though this reduction reached the statistical significance only in T-high vs. Control (Fig. 7). Creatinine levels were instead unchanged by pharmacological treatment (0.24 ± 0.19% in Control, 0.21 ± 0.09% in T-low and 0.29 ± 0.14% in T-high with p = 0.48).

Tgfb1 (Transforming Growth Factor Beta 1) expression was reduced, with respect to Control, in both T-low (-28%, p = 0.006) and T-high (−26%, p = 0.003) (Fig. 8). Likewise, Il6 (Interleukin-6) expression was reduced vs Control, in both T-low (-66%, p = 0.02) and T-high

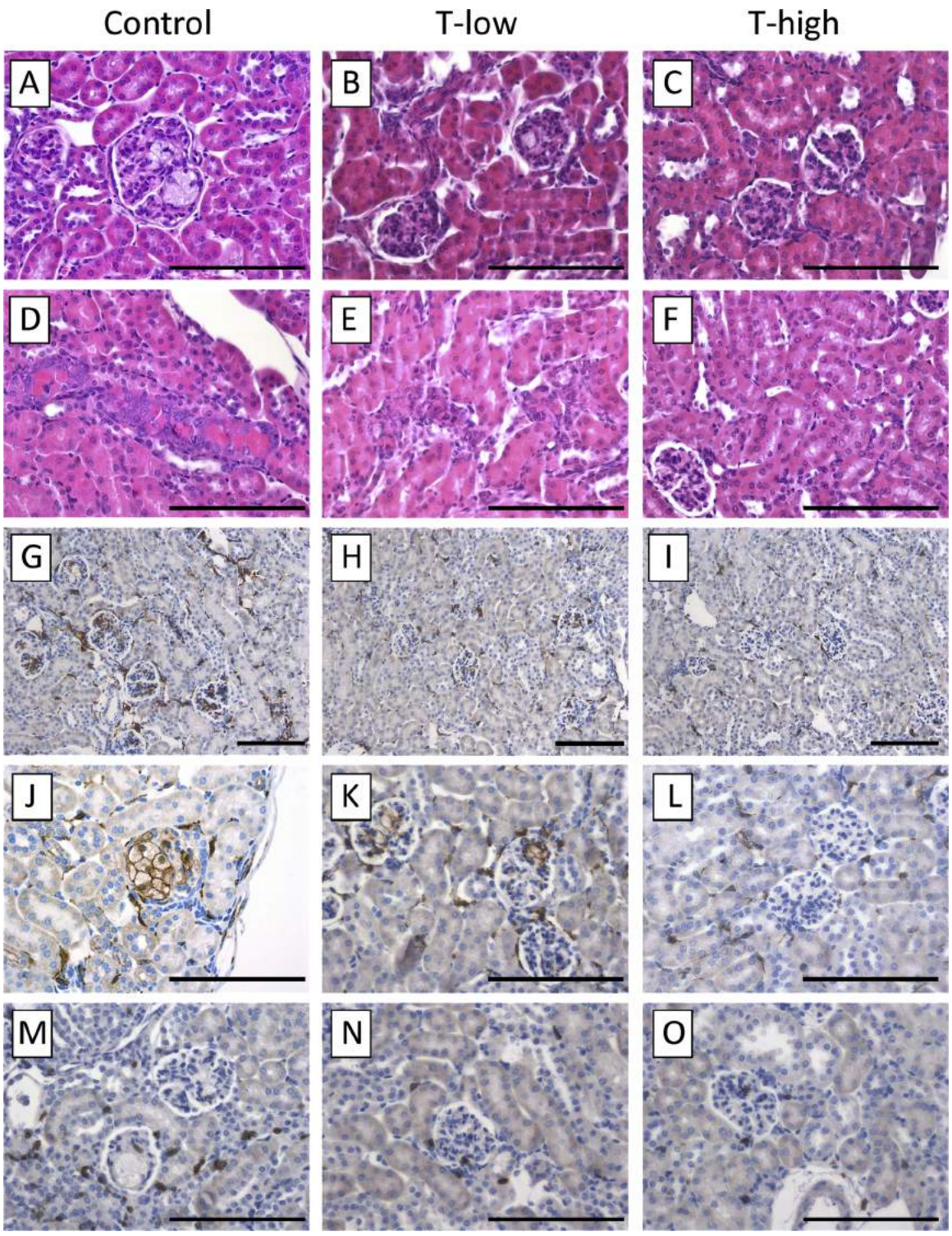

Fig. 6. Representative photomicrographs of kidney. H&E images of renal parenchyma show a progressive reduction of glomerular lipidosis from Control (**A**) to T-low (**B**) and T-high (**C**) and a similar trend for the presence of tubular necrosis in Control (**D**), T-low (**E**) and T-high (**F**). Iba-1 immunostaining highlights the macrophagic origin of foam cells within glomeruli (low magnification **G**, **H**, **I** and high magnification J, **K**, **L**). CD3 immunostaining showed a slight increase in T cells in renal parenchyma of Control compared to the others (**M**, **N**, **O**). Bar length = 100 μm.

(−56%, p = 0.008). Ccl2 (also known as MCP-1, monocyte chemoattractant protein-1) was also reduced, compared to Control, in both T-low (-64%, p = 0.006) and T-high (−60%, p = 0.003) (Fig. 8).

4. Discussion

The main result of the present study is that topiramate treatment showed a protective effect against kidney injury in apoE-deficient mice. The study was aimed at investigating a possible effect of topiramate on atherosclerosis development and related injuries at target organs of altered metabolic conditions. The apoE–deficient mouse model was chosen because it develops spontaneous hypercholesterolemia and arterial lesions that, similarly to those observed in humans, progress from early fatty streaks to advanced lesions, with the formation of a fibrous

Table 2
Kidney histological features.

Control		T-low		T-high	
Glomerular lipidosi	Tubular necrosis	Glomerular lipidosis	Tubular necrosis	Glomerular lipidosis	Tubular necrosis
3	0	0	0	2	0
3	0	1	0	1	0
2	0	1	0	0	0
3	0	2	0	3	0
3	0	1	0	2	0
3	1	2	0	1	0
3	1	2	1	0	0
3	0	2	0	1	0
3	1	1	0	2	0
		3	0	0	0

In the kidney, glomerular lipidosis was evaluated as the number of glomeruli affected per area and ranked as follows: 0: no glomeruli affected; 1: 1–3 glomeruli affected; 2: 4–10 glomeruli affected; 3: 11 or more glomeruli affected. Tubular necrosis was scored as present (1) or absent (0).

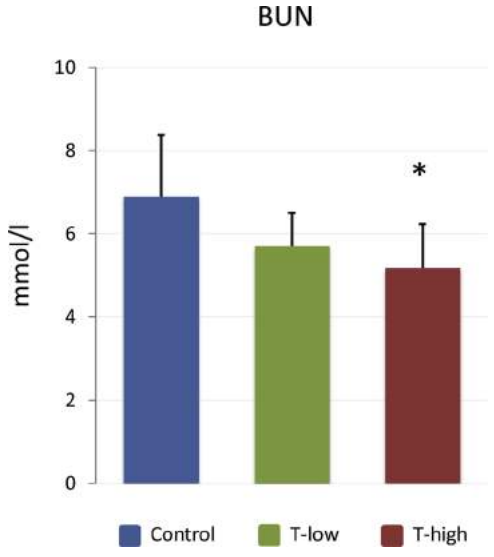

Fig. 7. Blood urea nitrogen (BUN) was measured in plasma and showed significantly lower levels in T-high vs Control (*p = 0.016). Data are expressed as mean ± SD. Significant differences were determined by one-way ANOVA followed by Tukey's post hoc test.

cap and a necrotic lipid core [22,23]. When fed a high fat, cholesterol-containing diet, apoE-deficient mice show increased hypercholesterolemia and accelerated atherosclerosis development [22,23]. In addition, this dietary treatment leads to altered glucose metabolism [24,25]. Hypercholesterolemia is a well-known risk factor for atherosclerosis development and it is also considered a contributing factor towards the development of renal dysfunction in the clinic [26]. In apoE-deficient mice, dyslipidemia-related kidney injury develops [27,28] and is characterized by marked pathological alterations that include foam cell accumulation and lipid deposits in glomerular capillaries termed "lipoprotein thrombi". The latter feature is typically found in lipoprotein glomerulopathy, a renal condition associated to specific apoE mutations in humans [29,30].

Topiramate was administered at the maximal effective and non-toxic dose described for mice [31], and at a lower dose, also used in previous experimental studies [32].

In the present study, possible effects of topiramate on body weight, glucose metabolism and lipid levels were investigated. The treatment did not significantly affect food intake as well as body weight, although a slightly lower weight gain was observed in the T-high group compared with Control. No significant differences among groups were also found in abdominal fat weight and histology. The weight loss induced in the clinic by topiramate treatment appears to be significant only in overweight and obese patients, whereas in experimental studies it seems to be strongly dependent on the model used and the duration of treatment [10,33]. Being the present study designed in young, growing mice, and for a relatively short duration of time, a lack of effect on body weight in this study is not surprising. Indeed, previous studies in the same experimental conditions have shown that apoE-deficient mice do not develop an obese phenotype [15,16,34].

A dose-dependent increase in water intake was observed in topiramate-treated mice vs Control. To our knowledge, this effect by topiramate treatment has not been described in the clinic, nor in other experimental studies. Being the increased water intake started just after the beginning of treatment, it should not be a consequence of possible biochemical or metabolic changes caused by topiramate. Although speculative, it could be simply due to the unpleasant taste of topiramate-containing food. Indeed, topiramate is known for its bitterness that, especially in paediatric patients, represents the greatest barrier to completion of treatment [35].

Topiramate treatment did not modify plasma cholesterol and triglyceride levels, as well as baseline glycaemia and response to glucose challenge. In the clinic, beneficial effects by topiramate on glycaemic control and lipid levels have generally been observed in association with weight loss [36,37]. In the few experimental studies that have addressed this issue, results seem to be related to the animal models used. In wild-type and diabetic rats a reduction of glucose and lipid levels was observed [38,39], whereas in mice the metabolic effects of topiramate seem to be strongly dependent on the diet and the genotype [31,33].

One of the main objectives of the present study was the evaluation of a possible effect by topiramate on atherosclerosis development. Disappointingly, the pharmacological treatment did not modify the extent of atherosclerotic lesions, both at the entire aorta and at the aortic sinus. This result may be at least partially explained by a lack of changes by treatment of the extremely elevated plasma cholesterol levels that characterize this mouse model.

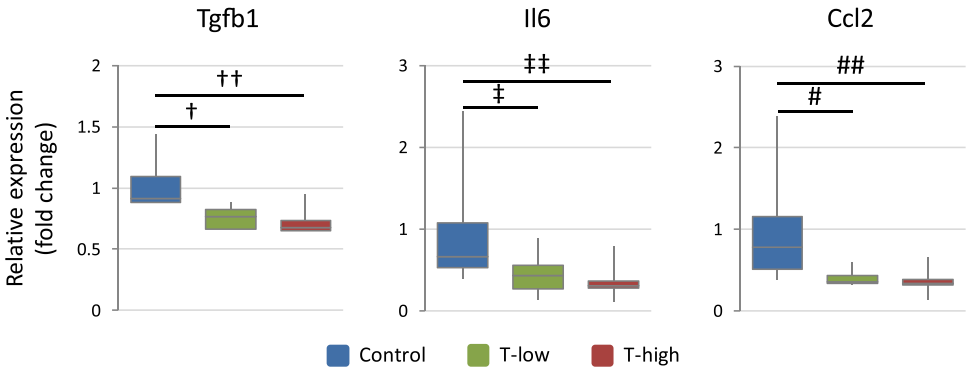

Fig. 8. Box plots of gene expression in the kidney of Control and topiramate-treated groups. Fold changes of renal genes, relative to Control group, are charted. The expression of Tgfb1, Il6 and Ccl2 were significantly reduced by treatment ($^{\dagger}p = 0.006$; $^{\dagger\dagger}p = 0.003$; $^{\ddagger}p = 0.02$; $^{\ddagger\ddagger}p = 0.008$; $^{\#}p = 0.006$; $^{\#\#}p = 0.003$). The upper and lower ends of the boxes indicate the 25th and 75th percentiles, respectively. The length of the box depicts the interquartile range within which 50% of the values are located. The solid gray lines identify the median. Significant differences were determined by one-way ANOVA followed Tukey's post hoc test.

Topiramate treatment did not affect glycogen and lipid accumulation in the hepatic cells, as well as the amount of subendothelial foamy macrophages. Conversely, histological analysis of kidneys showed that topiramate strongly reduced the accumulation of foam cells in glomeruli, which were of macrophagic origin. This alteration has been described in apoE-deficient mice fed both chow and high fat diet [27,28,40]. In humans, foam cells accumulation is a feature of glomerular lipidosis associated to dyslipidemic conditions, such as type III hyperlipoproteinemia and LCAT deficiency [29,41,42], both prone to the development of kidney disease [30,43].

It is unlikely that the reduction of foam cell formation could be a consequence of a reduced accumulation of lipids in the glomerulus, since topiramate treatment did not modify plasma lipids. Alternatively, topiramate could have interfered with foam cell formation by reducing macrophage uptake of modified lipoproteins. It is known that macrophages, as well as other cells of the immune system express GABA receptors [44] and that topiramate, among its several mechanisms of action, is a GABA-A receptor agonist [45]. In a previously published paper, this issue was investigated exposing human monocyte-derived macrophages (HMDM) to oxidised LDL in the absence or presence of topiramate. Topiramate was shown to markedly reduce lipid droplets accumulation and the cholesterol content in HMDM, indicating that GABA-A receptor stimulation, one of the mechanisms of action of topiramate, exerts inhibitory effects on phagocytic activity for oxidized LDL [46]. This result is consistent with previous observations relating GABA receptor stimulation with alterations of monocyte/macrophage activity [47].

In this study the most abundant presence of foamy macrophages in Control was associated with an increased expression of Il6 and Ccl2/Mcp-1, indicative of an increased inflammatory milieu within the kidney parenchyma. A causative role of glomerular foam cells accumulation in impaired renal function has not been yet fully established [48]. In the present study, plasma BUN and creatinine levels were in the normal range in all the three groups of mice [49]. It is known that BUN and creatinine levels rise dramatically only when more than 50% of renal function is compromised [50,51]. However, fluctuations of these parameters within the physiological range still reflect changes in the glomerular filtration rate [50]. In the present study topiramate treatment significantly reduced BUN levels, whereas creatinine concentration was unchanged by treatment. This is consistent with previous studies in mice where BUN is subjected to broader fluctuations than creatinine [52,53]. Thus, a possible protective effect of topiramate on kidney function cannot be excluded. In accordance, Tgfb1 expression, which is upregulated in response to harmful stimuli and leads to impaired glomerular filtration [54], was significantly reduced after topiramate treatment.

It is well known that macrophage-derived foam cells are a relevant component of atherosclerotic plaques both in humans and in apoE-deficient mice [23,55]. In the present study the accumulation of macrophages and foam cells in plaques developing at the aortic sinus was not different among controls and topiramate-treated mice. This result was unexpected, based on the reduction of foam cells in glomeruli caused by treatment. This discrepancy may reside in the different features of the two anatomical sites. Macrophages in atheromas mostly derive from circulating blood monocytes, since healthy arterial walls do not harbour resident phagocytes [56]. Conversely, in kidneys, there is a small population of tissue-resident macrophages that are predominantly derived from embryonic macrophages [57]. Besides oxidised lipoproteins, atheromas are filled with potent pro-inflammatory stimuli, such as cellular debris coming from disintegrating macrophages and neutrophils, as well as chemokines and cytokines produced by trapped leukocytes [58]. The conditions within the plaque are so extreme that the plaque core is not populated with live cells, as the compact nature of the plaque renders the diffusion of molecules, oxygen and nutrients extremely difficult [59]. On the contrary, the glomerulus is, by the means of its function, filled with capillaries, with opposite conditions than those found in atherosclerotic plaques. Reportedly, the origin and activation state of the macrophages and the microenvironment in which they reside are critical determinants of their response to injury [56,57].

Further, foam cell population in atherosclerotic lesions does not entirely derive from macrophages. Multiple studies have in fact demonstrated that foam cells in atherosclerotic plaques, although expressing typical macrophage markers, are smooth muscle cells derived [60,61]. Finally, it cannot be excluded that the protective effect by topiramate against foam cells accumulation may have been overcome by the severe hyperlipidemia that strongly drives atherosclerotic plaque formation in apoE-deficient mice fed high fat diet [23].

Being topiramate an inhibitor of carbonic anhydrases, about 1.5% of adult patients treated with this drug may develop nephrolithiasis and its incidence increases in the paediatric population [62]. Although this effect by treatment was not specifically addressed, histological features seem to exclude this event. The increased water intake observed in topiramate-treated animals and the relatively short time frame of the experiment may have accounted for the lack in the incidence of this adverse effect.

5. Conclusions

In summary, topiramate treatment to apoE-deficient mice displayed a protective effect against glomerular lipidosis. This condition, described in dyslipidemic patients that are prone to develop kidney disease, is currently without therapeutic options. Considering the wide use of this drug in the general population, these results are particularly relevant and potentially open a new scenario in the treatment of this clinical condition.

Author contributions

S.M., M.B., L.M., A.O., E.B., S.S., E.S., performed the experiments, S.M., M.B., C.P., E.S., G.C. analyzed and interpreted the data, S.M., M.B., A.P., E.L., G.C., conceived the project, S.M., M.B., G.C. designed the study and wrote the manuscript, G.C. supervised the research.

All authors gave final approval of the current version of the article being submitted.

Declaration of interest

Andreas Persidis is CEO and Eftychia Lekka is senior investigator at Biovista, Athens, Greece. All other authors declare no competing interests.

Acknowledgements

This work was funded by the European Community's Seventh Framework Programme (FP7/2012–2017) RiskyCAD, grant no. 305739 (G.C.), by Fondazione CARIPLO (2011-0645) (G.C.) and by grants from MIUR Progetto Eccellenza. We are grateful to Ms. Elda Desiderio Pinto for administrative assistance. Part of this work was carried out at NOLIMITS, an advanced imaging facility established by the Università degli Studi di Milano

Appendix A. Supplementary data

Supplementary material related to this article can be found, in the online version, at doi:https://doi.org/10.1016/j.phrs.2018.12.022.

References

[1] V. Biton, G.D. Montouris, F. Ritter, J.J. Riviello, R. Reife, P. Lim, G. Pledger, A randomized, placebo-controlled study of topiramate in primary generalized tonic-clonic seizures. Topiramate YTC Study Group, Neurology 52 (1999) 1330–1337 http://prx.library.gatech.edu/login?url=http://search.ebscohost.com/login.aspx?

direct=true&db=mnh&AN=10227614&site=ehost-live.
[2] R.C. Sachdeo, T.A. Glauser, F. Ritter, R. Reife, P. Lim, G. Pledger, A double-blind, randomized trial of topiramate in Lennox-Gastaut syndrome. Topiramate YL Study Group, Neurology 52 (1999) 1882–1887 http://www.ncbi.nlm.nih.gov/pubmed/10371538.
[3] I.W. Tremont-Lukats, C. Megeff, M.M. Backonja, Anticonvulsants for neuropathic pain syndromes: mechanisms of action and place in therapy, Drugs 60 (2000) 1029–1052, https://doi.org/10.2165/00003495-200060050-00005.
[4] M.-M. Backonja, Use of anticonvulsants for treatment of neuropathic pain, Neurology 59 (2002) S14–7, https://doi.org/10.1212/WNL.59.5_suppl_2.S14.
[5] E. Spina, G. Perugi, Antiepileptic drugs: indications other than epilepsy, Epileptic Disord. 6 (2004) 57–75 http://www.ncbi.nlm.nih.gov/pubmed/15246950.
[6] D. Magis, J. Schoenen, Treatment of migraine: update on new therapies, Curr. Opin. Neurol. 24 (2011) 203–210, https://doi.org/10.1097/WCO.0b013e3283462c3f.
[7] M. Mula, Topiramate and cognitive impairment: evidence and clinical implications, Ther. Adv. Drug Saf. 3 (2012) 279–289, https://doi.org/10.1177/2042098612455357.
[8] E. Ben-Menachem, J.W. Sander, H. Stefan, S. Schwalen, B. Schäuble, Topiramate monotherapy in the treatment of newly or recently diagnosed epilepsy, Clin. Ther. 30 (2008) 1180–1195, https://doi.org/10.1016/j.clinthera.2005.02.013.
[9] S.D. Silberstein, E. Ben-Menachem, R.P. Shank, F. Wiegand, Topiramate monotherapy in epilepsy and migraine prevention, Clin. Ther. 27 (2005) 154–165, https://doi.org/10.1016/j.clinthera.2005.02.013.
[10] A. Verrotti, A. Scaparrotta, S. Agostinelli, S. Di Pillo, F. Chiarelli, S. Grosso, Topiramate-induced weight loss: a review, Epilepsy Res. 95 (2011) 189–199, https://doi.org/10.1016/j.eplepsyres.2011.05.014.
[11] R.P. Shank, J.F. Gardocki, A.J. Streeter, B.E. Maryanoff, An overview of the preclinical aspects of topiramate: pharmacology, pharmacokinetics, and mechanism of action, Epilepsia 41 (Suppl 1) (2000) S3–9, https://doi.org/10.1111/j.1528-1157.2000.tb02163.x.
[12] S. Tonstad, A. Tykarski, J. Weissgarten, A. Ivleva, B. Levy, A. Kumar, M. Fitchet, Efficacy and safety of topiramate in the treatment of obese subjects with essential hypertension, Am. J. Cardiol. 96 (2005) 243–251, https://doi.org/10.1016/j.amjcard.2005.03.053.
[13] A.N. Sweeting, E. Tabet, I.D. Caterson, T.P. Markovic, Management of obesity and cardiometabolic risk - role of phentermine/extended release topiramate, Diabetes Metab. Syndr. Obes. 7 (2014) 35–44, https://doi.org/10.2147/DMSO.S38979.
[14] M. Busnelli, S. Manzini, M. Hilvo, C. Parolini, G.S. Ganzetti, F. Dellera, K. Ekroos, M. Jänis, D. Escalante-Alcalde, C.R. Sirtori, R. Laaksonen, G. Chiesa, Liver-specific deletion of the Plpp3 gene alters plasma lipid composition and worsens atherosclerosis in apoE-/- mice, Sci. Rep. 7 (2017) 44503, https://doi.org/10.1038/srep44503.
[15] C. Parolini, R. Vik, M. Busnelli, B. Bjørndal, S. Holm, T. Brattelid, S. Manzini, G.S. Ganzetti, F. Dellera, B. Halvorsen, P. Aukrust, C.R. Sirtori, J.E. Nordrehaug, J. Skorve, R.K. Berge, G. Chiesa, A salmon protein hydrolysate exerts lipid-independent anti-atherosclerotic activity in ApoE-deficient mice, PLoS One 9 (2014) e97598, , https://doi.org/10.1371/journal.pone.0097598.
[16] C. Parolini, B. Bjorndal, M. Busnelli, S. Manzini, G.S. Ganzetti, F. Dellera, M. Ramsvik, I. Bruheim, R.K. Berge, G. Chiesa, Effect of dietary components from Antarctic Krill on atherosclerosis in apoE-Deficient mice, Mol. Nutr. Food Res. 61 (2017) 1700098, , https://doi.org/10.1002/mnfr.201700098.
[17] C.A. Schneider, W.S. Rasband, K.W. Eliceiri, NIH Image to ImageJ: 25 years of image analysis, Nat. Methods 9 (2012) 671–675, https://doi.org/10.1038/nmeth.2089.
[18] Š. Lhoták, G. Gyulay, J.-C. Cutz, A. Al-Hashimi, B.L. Trigatti, C.D. Richards, S.A. Igdoura, G.R. Steinberg, J. Bramson, K. Ask, R.C. Austin, Characterization of proliferating lesion-resident cells during all stages of atherosclerotic growth, J. Am. Heart Assoc. 5 (2016) 27528409, , https://doi.org/10.1161/JAHA.116.003945.
[19] S. Manzini, C. Pinna, M. Busnelli, P. Cinquanta, E. Rigamonti, G.S. Ganzetti, F. Dellera, A. Sala, L. Calabresi, G. Franceschini, C. Parolini, G. Chiesa, Beta2-adrenergic activity modulates vascular tone regulation in lecithin:cholesterol acyltransferase knockout mice, Vascul. Pharmacol. 74 (2015) 114–121, https://doi.org/10.1016/j.vph.2015.08.006.
[20] K.J. Livak, T.D. Schmittgen, Analysis of relative gene expression data using real-time quantitative PCR and the 2(-Delta Delta C(T)) Method, Methods 25 (2001) 402–408, https://doi.org/10.1006/meth.2001.1262.
[21] X. Cui, J. Zhou, J. Qiu, M.R. Johnson, M. Mrug, Validation of endogenous internal real-time PCR controls in renal tissues, Am. J. Nephrol. 30 (2009) 413–417, https://doi.org/10.1159/000235993.
[22] A.S. Plump, J.D. Smith, T. Hayek, K. Aalto-Setälä, A. Walsh, J.G. Verstuyft, E.M. Rubin, J.L. Breslow, Severe hypercholesterolemia and atherosclerosis in apolipoprotein E-deficient mice created by homologous recombination in ES cells, Cell 71 (1992) 343–353, https://doi.org/10.1016/0092-8674(92)90362-G.
[23] Y. Nakashima, A.S. Plump, E.W. Raines, J.L. Breslow, R. Ross, ApoE-deficient mice develop lesions of all phases of atherosclerosis throughout the arterial tree, Arterioscler. Thromb. a J. Vasc. Biol. 14 (1994) 133–140, https://doi.org/10.1161/01.ATV.14.1.133.
[24] Z. Su, Y. Li, J.C. James, A.H. Matsumoto, G.A. Helm, A.J. Lusis, W. Shi, Genetic linkage of hyperglycemia, body weight and serum amyloid-P in an intercross between C57BL/6 and C3H apolipoprotein E-deficient mice, Hum. Mol. Genet. 15 (2006) 1650–1658, https://doi.org/10.1093/hmg/ddl088.
[25] J. Li, Q. Wang, W. Chai, M.-H. Chen, Z. Liu, W. Shi, Hyperglycemia in apolipoprotein E-deficient mouse strains with different atherosclerosis susceptibility, Cardiovasc. Diabetol. 10 (2011) 117, https://doi.org/10.1186/1475-2840-10-117.
[26] P. Muntner, J. Coresh, J.C. Smith, J. Eckfeldt, M.J. Klag, Plasma lipids and risk of developing renal dysfunction: the atherosclerosis risk in communities study, Kidney Int. 58 (2000) 293–301, https://doi.org/10.1046/j.1523-1755.2000.00165.x.
[27] M. Wen, S. Segerer, M. Dantas, P.A. Brown, K.L. Hudkins, T. Goodpaster, E. Kirk, R.C. LeBoeuf, C.E. Alpers, Renal injury in apolipoprotein E-deficient mice, Lab. Invest. 82 (2002) 999–1006 http://www.ncbi.nlm.nih.gov/pubmed/12177238.
[28] S.S. Carneiro, R.Z. Carminati, F.P.S. Freitas, P.L. Podratz, C.M. Balarini, J.B. Graceli, S.S. Meyrelles, E.C. Vasquez, A.L. Gava, Endogenous female sex hormones delay the development of renal dysfunction in apolipoprotein E-deficient mice, Lipids Health Dis. 13 (2014) 176, https://doi.org/10.1186/1476-511X-13-176.
[29] H. Sato, N. Takahashi, E. Sato, K. Kisu, S. Ito, T. Saito, Pathology of glomerular lipidosis, Clin. Exp. Nephrol. 18 (2014) 194–196, https://doi.org/10.1007/s10157-013-0882-9.
[30] T. Saito, A. Matsunaga, S. Oikawa, Impact of lipoprotein glomerulopathy on the relationship between lipids and renal diseases, Am. J. Kidney Dis. 47 (2006) 199–211, https://doi.org/10.1053/j.ajkd.2005.10.017.
[31] Y. Liang, X. Chen, M. Osborne, S.O. DeCarlo, T.L. Jetton, K. Demarest, Topiramate ameliorates hyperglycaemia and improves glucose-stimulated insulin release in ZDF rats and db/db mice, Diabetes Obes. Metab. 7 (2005) 360–369, https://doi.org/10.1111/j.1463-1326.2004.00403.x.
[32] C.P. Coomans, J.J. Geerling, S.A.A. van den Berg, H.C. van Diepen, N. Garcia-Tardón, A. Thomas, J.P. Schröder-van der Elst, D.M. Ouwens, H. Pijl, P.C.N. Rensen, L.M. Havekes, B. Guigas, J.A. Romijn, The insulin sensitizing effect of topiramate involves KATP channel activation in the central nervous system, Br. J. Pharmacol. 170 (2013) 908–918, https://doi.org/10.1111/bph.12338.
[33] J. Lalonde, P. Samson, S. Poulin, Y. Deshaies, D. Richard, Additive effects of leptin and topiramate in reducing fat deposition in lean and obese ob/ob mice, Physiol. Behav. 80 (2004) 415–420, https://doi.org/10.1016/j.physbeh.2003.08.013.
[34] R. Vik, M. Busnelli, C. Parolini, B. Bjørndal, S. Holm, P. Bohov, B. Halvorsen, T. Brattelid, S. Manzini, G.S. Ganzetti, F. Dellera, O.K. Nygård, P. Aukrust, C.R. Sirtori, G. Chiesa, R.K. Berge, An immunomodulating fatty acid analogue targeting mitochondria exerts anti-atherosclerotic effect beyond plasma cholesterol-lowering activity in apoe(-/-) mice, PLoS One 8 (2013) e81963, , https://doi.org/10.1371/journal.pone.0081963.
[35] T. Haraguchi, T. Uchida, M. Hazekawa, M. Yoshida, M. Nakashima, H. Sanda, T. Hase, Y. Tomoda, Ability of Food/Drink to reduce the bitterness intensity of topiramate as determined by taste sensor analysis, Chem. Pharm. Bull. (Tokyo) 64 (2016) 14–20, https://doi.org/10.1248/cpb.c15-00474.
[36] E. Ben-Menachem, M. Axelsen, E.H. Johanson, A. Stagge, U. Smith, Predictors of weight loss in adults with topiramate-treated epilepsy, Obes. Res. 11 (2003) 556–562, https://doi.org/10.1038/oby.2003.78.
[37] H. Li, Y. Zou, Z. Xia, F. Gao, J. Feng, C. Yang, Effects of topiramate on weight and metabolism in children with epilepsy, Acta Paediatr. 98 (2009) 1521–1525, https://doi.org/10.1111/j.1651-2227.2009.01349.x.
[38] Y. Liang, P. She, X. Wang, K. Demarest, The messenger RNA profiles in liver, hypothalamus, white adipose tissue, and skeletal muscle of female Zucker diabetic fatty rats after topiramate treatment, Metabolism 55 (2006) 1411–1419, https://doi.org/10.1016/j.metabol.2006.06.013.
[39] H.S. El-Abhar, M.F. Schaalan, Topiramate-induced modulation of hepatic molecular mechanisms: an aspect for its anti-insulin resistant effect, PLoS One 7 (2012) e37757, , https://doi.org/10.1371/journal.pone.0037757.
[40] Z. Pei, T. Okura, T. Nagao, D. Enomoto, M. Kukida, A. Tanino, K.-I. Miyoshi, M. Kurata, J. Higaki, Osteopontin deficiency reduces kidney damage from hypercholesterolemia in Apolipoprotein E-deficient mice, Sci. Rep. 6 (2016) 28882, , https://doi.org/10.1038/srep28882.
[41] T. Saito, Abnormal lipid metabolism and renal disorders, Tohoku J. Exp. Med. 181 (1997) 321–337, https://doi.org/10.1620/tjem.181.321.
[42] K. Suzaki, S. Kobori, S. Ueno, M. Uehara, T. Kayashima, H. Takeda, S. Fukuda, K. Takahashi, N. Nakamura, H. Uzawa, Effects of plasmapheresis on familial type III hyperlipoproteinemia associated with glomerular lipidosis, nephrotic syndrome and diabetes mellitus, Atherosclerosis 80 (1990) 181–189, https://doi.org/10.1016/0021-9150(90)90025-E.
[43] M. Gigante, E. Ranieri, G. Cerullo, L. Calabresi, A. Iolascon, G. Assmann, L. Morrone, L. Pisciotta, F.P. Schena, L. Gesualdo, LCAT deficiency: molecular and phenotypic characterization of an Italian family, J. Nephrol. 19 (2006) 375–381 http://www.ncbi.nlm.nih.gov/pubmed/16874701.
[44] R. Bhat, R. Axtell, A. Mitra, M. Miranda, C. Lock, R.W. Tsien, L. Steinman, Inhibitory role for GABA in autoimmune inflammation, Proc. Natl. Acad. Sci. U. S. A. 107 (2010) 2580–2585, https://doi.org/10.1073/pnas.0915139107.
[45] H.S. White, S.D. Brown, J.H. Woodhead, G.A. Skeen, H.H. Wolf, Topiramate enhances GABA-mediated chloride flux and GABA-evoked chloride currents in murine brain neurons and increases seizure threshold, Epilepsy Res. 28 (1997) 167–179, https://doi.org/10.1016/S0920-1211(97)00045-4.
[46] Y. Yang, Y.-T. Lian, S.-Y. Huang, Y. Yang, L.-X. Cheng, K. Liu, GABA and topiramate inhibit the formation of human macrophage-derived foam cells by modulating cholesterol-metabolism-associated molecules, Cell. Physiol. Biochem. 33 (2014) 1117–1129, https://doi.org/10.1159/000358681.
[47] Y. Yang, H. Luo, L.-X. Cheng, K. Liu, Inhibitory role for GABA in atherosclerosis, Med. Hypotheses 81 (2013) 803–804, https://doi.org/10.1016/j.mehy.2013.08.029.
[48] M. Eom, K.L. Hudkins, C.E. Alpers, Foam cells and the pathogenesis of kidney disease, Curr. Opin. Nephrol. Hypertens. 24 (2015) 245–251, https://doi.org/10.1097/MNH.0000000000000112.
[49] P. Meneton, I. Ichikawa, T. Inagami, J. Schnermann, Renal physiology of the mouse, Am. J. Physiol. Renal Physiol. 278 (2000) F339–F351, https://doi.org/10.1152/ajprenal.2000.278.3.F339.
[50] K.H. Walker, D.W. Hall, W.J. Hurst, Clinical methods: the history, physical, and laboratory examinations, Clin. Methods Hist. Phys. Lab. Exam. 3rd editio,

Butterworths, Boston, Boston, 1990, p. 1087.
[51] J.E. Harkness, P.V. Turner, S. VandeWoude, C.L. Wheler, Harkness and Wagner's Biology and Medicine of Rabbits and Rodents, fifth edit, Wiley-Blackwell, 1995, p. 436.
[52] S.K. Kesavan, S. Bhat, S.B. Golegaonkar, M.G. Jagadeeshaprasad, A.B. Deshmukh, H.S. Patil, S.D. Bhosale, M.L. Shaikh, H.V. Thulasiram, R. Boppana, M.J. Kulkarni, Proteome wide reduction in AGE modification in streptozotocin induced diabetic mice by hydralazine mediated transglycation, Sci. Rep. 3 (2013) 2941, https://doi.org/10.1038/srep02941.
[53] L.J. Stallons, R.M. Whitaker, R.G. Schnellmann, Suppressed mitochondrial biogenesis in folic acid-induced acute kidney injury and early fibrosis, Toxicol. Lett. 224 (2014) 326–332, https://doi.org/10.1016/j.toxlet.2013.11.014.
[54] A. Ghayur, P.J. Margetts, Transforming growth factor-beta and the glomerular filtration barrier, Kidney Res. Clin. Pract. 32 (2013) 3–10, https://doi.org/10.1016/j.krcp.2013.01.003.
[55] X.-H. Yu, Y.-C. Fu, D.-W. Zhang, K. Yin, C.-K. Tang, Foam cells in atherosclerosis, Clin. Chim. Acta 424 (2013) 245–252, https://doi.org/10.1016/j.cca.2013.06.006.
[56] S. Gordon, A. Plüddemann, Tissue macrophages: heterogeneity and functions, BMC Biol. 15 (2017) 53, https://doi.org/10.1186/s12915-017-0392-4.
[57] D.A.D. Munro, J. Hughes, The origins and functions of tissue-resident macrophages in kidney development, Front. Physiol. 8 (2017) 1–13, https://doi.org/10.3389/fphys.2017.00837.
[58] C. Kasikara, A.C. Doran, B. Cai, I. Tabas, The role of non-resolving inflammation in atherosclerosis, J. Clin. Invest. 128 (2018) 2713–2723, https://doi.org/10.1172/JCI97950.
[59] J.F. Bentzon, F. Otsuka, R. Virmani, E. Falk, Mechanisms of plaque formation and rupture, Circ. Res. 114 (2014) 1852–1866, https://doi.org/10.1161/CIRCRESAHA.114.302721.
[60] J.A. Dubland, G.A. Francis, So much cholesterol: the unrecognized importance of smooth muscle cells in atherosclerotic foam cell formation, Curr. Opin. Lipidol. 27 (2016) 155–161, https://doi.org/10.1097/MOL.0000000000000279.
[61] A.L. Durham, M.Y. Speer, M. Scatena, C.M. Giachelli, C.M. Shanahan, Role of smooth muscle cells in vascular calcification: implications in atherosclerosis and arterial stiffness, Cardiovasc. Res. 114 (2018) 590–600, https://doi.org/10.1093/cvr/cvy010.
[62] S.M. Barnett, A.H. Jackson, B.A. Rosen, J.L. Garb, G.L. Braden, Nephrolithiasis and nephrocalcinosis from topiramate therapy in children with epilepsy, Kidney Int. Rep. 3 (2018) 684–690, https://doi.org/10.1016/j.ekir.2018.02.005.